Available online at www.sciencedirect.com

ScienceDirect

Journal of Computational and Applied Mathematics 206 (2007) 454–472

JOURNAL OF COMPUTATIONAL AND APPLIED MATHEMATICS

www.elsevier.com/locate/cam

On the use of Hadamard expansions in hyperasymptotic evaluation of Laplace-type integrals—IV: Poles

R.B. Paris*

Division of Complex Systems, University of Abertay Dundee, Dundee DD1 1HG, UK

Received 31 May 2006; received in revised form 9 August 2006

Abstract

This paper is one of a series considering the application of Hadamard expansions in the hyperasymptotic evaluation of Laplace-type integrals of the form $\int_C \exp\{-z\psi(t)\} f(t)\,\mathrm{d}t$ for large values of $|z|$. It is shown how the procedure can be employed to deal with the case when the amplitude function $f(t)$ possesses poles which may coalesce with a saddle point of the integrand or approach the integration path C. A novel feature introduced here is the *reverse-expansion procedure*. This results in contributions at each exponential level (after the first) of the expansion in the form of rapidly convergent series, thereby enabling the high-precision evaluation of the above integral in coalescence problems. Numerical examples are given to illustrate the procedure.

Keywords: Asymptotics; Hyperasymptotics; Hadamard expansions; Laplace-type integrals

1. Introduction

This is the final paper in a sequence of papers [10–12] (hereinafter referred to as I, II and III) dealing with the hyperasymptotic evaluation[1] of Laplace-type integrals of the form

$$J(z) = \int_C \mathrm{e}^{-z\psi(t)}\, f(t)\,\mathrm{d}t \tag{1.1}$$

for large values of $|z|$ by means of Hadamard expansions. In the most general case, the phase function $\psi(t)$ possesses saddle points (given by the points where $\psi'(t) = 0$) and the integration path C, which may be finite or infinite in extent, is supposed to coincide with a path of steepest descent through a particular saddle point labelled t_s. The amplitude function $f(t)$ possesses poles (or branch-point singularities) which either remain static in the complex t-plane, or which may coalesce with saddle points or approach the integration path C as some parameter varies.

In I and II the cases of real and complex values of z were considered, together with a discussion of how the Hadamard expansion procedure could be modified to deal with the calculation of (1.1) in the presence of a Stokes phenomenon. In III, the Hadamard expansion procedure was extended to deal with clusters of saddle points of the phase function which

* Tel.:+44 1382 380618; fax: +44 1382 308161.
E-mail address: r.paris@abertay.ac.uk.

[1] By hyperasymptotic evaluation is meant, in the broadest sense, any means of evaluation that achieves an accuracy greater than that obtainable by optimal truncation of an asymptotic expansion.

0377-0427/$ - see front matter © 2006 Published by Elsevier B.V.
doi:10.1016/j.cam.2006.08.016

can undergo coalescence as a parameter in $\psi(t)$ approaches a critical value. Other examples dealing with coalescence of saddles with endpoints of the integration path, and in the context of the Bessel functions of large order and argument and Pearcey's integral, have been given in [9,13,14]. We point out that the use of Hadamard expansions in a non-asymptotic setting has been recently discussed in [5,17] and in numerical schemes for the evaluation of Kummer functions and the exponential integral in [2,6,7].

A Hadamard expansion is a series of the form[2]

$$S_n(z) = \sum_{k=0}^{\infty} \frac{c_{kn}}{(\omega_n z)^{\alpha_n k+\beta_n}} P(\alpha_n k + \beta_n, \omega_n|z|), \tag{1.2}$$

where c_{kn} are coefficients that result from expansion of the integrand of (1.1) about a suitably chosen sequence of points labelled by the integer n. The quantities ω_n measure the lengths of the intervals in the subdivision of the image of the path C in the Borel plane and α_n, β_n are positive parameters that depend on the order of the saddle and whether it is an endpoint or otherwise of the nth interval. The function $P(a, x)$ denotes the normalised incomplete gamma function

$$\begin{aligned} P(a,x) &= \frac{\gamma(a,x)}{\Gamma(a)} = \frac{1}{\Gamma(a)} \int_0^x \mathrm{e}^{-t} t^{a-1}\,\mathrm{d}t \quad (|\arg x| < \pi,\ \mathrm{Re}(a) > 0) \\ &= \frac{x^a \mathrm{e}^{-x}}{\Gamma(1+a)} {}_1F_1(1; 1+a; x), \end{aligned} \tag{1.3}$$

where ${}_1F_1$ is the confluent hypergeometric function. Due to their cut-off nature in k for large $\omega_n|z|$, the incomplete gamma functions in (1.2) act as a smoothing factor, thereby ensuring that the Hadamard series $S_n(z)$ is absolutely convergent (subject possibly to some restriction on β_n), rather than asymptotic; see I.

In I–III, it was shown that, in the case of the path C emanating from a saddle point t_s, $J(z)$ could be expressed exactly in the form

$$J(z) = \mathrm{e}^{-z\psi(t_s)} \sum_n \mathrm{e}^{-\Omega_n|z|} S_n(z), \tag{1.4}$$

where the number of levels n may be finite or infinite depending on whether the path C is finite or infinite. The quantities Ω_n are termed the *exponential levels* of the expansion and are related to the interval lengths ω_n by the relation $\Omega_n = \sum_{r=0}^{n-1} \omega_r$ $(n \geqslant 1)$, with $\Omega_0 = 0$. We consider two basic methods of selecting the ω_n. The first, which we call herein the *forward-expansion procedure* and which has been employed in I–III, consists of choosing ω_n to be the radii of convergence of the expansion of the integrand of (1.1) about the left-hand endpoints Ω_n of the intervals in the subdivision of the path C in the Borel plane. This choice has the advantage of maximising the exponential separation between the different levels in (1.4), but results in each Hadamard series (1.2) requiring modification (achieved by a simple re-arrangement of the terms in its tail) to produce a rapidly decaying series when $|z|$ is large. The second method, which we call the *reverse-expansion procedure*, consists of expanding about the right-hand endpoints of the intervals whose lengths (when $n \geqslant 1$) may be suitably chosen. Such a procedure results in the Hadamard series (1.2) with $n \geqslant 1$ possessing terms that decay rapidly without the need for the tail-rearrangement required in the first method. This method is of considerable interest since it avoids the necessity of computing the coefficients in the modified form of the Hadamard series, which is computationally the most expensive part of the process. A version of this approach, consisting of a combination of the reverse- and forward-expansion procedures, has been shown in [9,12,14] to be indispensable when dealing with coalescing saddle points.

The structure of the paper is as follows. In Section 2, we describe the Hadamard expansion procedure for the integral $J(z)$ in (1.1) and discuss the two methods of selection of the interval lengths ω_n in the Borel plane. In the remainder of the paper we discuss specific examples of Laplace-type integrals where the amplitude function $f(t)$ possesses poles

[2] The presence of the quantities ω_n in the denominator is optional since they also appear in the definition of the coefficients c_{kn}. Their absence is particularly appropriate when dealing with coalescence problems where $\omega_n \to 0$ and this will be the position we adopt in this paper.

that can coalesce with a saddle point or approach the integration path C. Numerical results are given in each case to illustrate the accuracy achievable with this procedure.

2. The Hadamard expansion process

We present a summary of the Hadamard expansion procedure for the Laplace-type integral in (1.1) when the integration path C, which may be finite or infinite in extent, is supposed to coincide with a path of steepest descent through a particular saddle point labelled t_s. With $\theta = \arg z$, the change of variable $u = \mathrm{e}^{\mathrm{i}\theta}\{\psi(t) - \psi(t_s)\}$ enables (1.1) to be cast in the form

$$J(z) = \mathrm{e}^{-z\psi(t_s)} \int_{C'} \mathrm{e}^{-|z|u} f(t) \frac{\mathrm{d}t}{\mathrm{d}u} \,\mathrm{d}u, \tag{2.1}$$

where C' is the image of the path C in the u-plane. If C is infinite in extent on both sides of t_s, passing to infinity along appropriate directions, then C' is the negatively orientated loop about $u = 0$ surrounding the positive real axis; if, on the other hand, C commences at t_s and passes to infinity then C' is an appropriate half of the loop.

The positive real u-axis is now subdivided into a series of intervals of length ω_n $(n = 0, 1, 2, \ldots)$ with left-hand endpoints at $u = \Omega_n$, where $\Omega_0 = 0$ and

$$\Omega_n = \sum_{r=0}^{n-1} \omega_r \quad (n \geqslant 1). \tag{2.2}$$

The corresponding endpoints on the path C in the t-plane are denoted by $t_0\,(\equiv t_s), t_1^{\pm}, t_2^{\pm}, \ldots$, where the '$\pm$' superscripts refer to the halves of C that emanate from and lead up to t_s, respectively; see Fig. 1. The values of $t_n^{\pm}$ are obtained by straightforward solution of the equation

$$\psi(t_n^{\pm}) - \psi(t_s) = \Omega_n \mathrm{e}^{-\mathrm{i}\theta} \quad (n \geqslant 1). \tag{2.3}$$

From the above definitions of u, ω_n and Ω_n, we have for arbitrary complex τ

$$\psi(t_n^{\pm} + \tau) - \psi(t_n^{\pm}) = (u - \Omega_n)\mathrm{e}^{-\mathrm{i}\theta} = \omega_n v \mathrm{e}^{-\mathrm{i}\theta} \quad (n \geqslant 0), \tag{2.4}$$

where the variable v is given by $u = \Omega_n + \omega_n v$, $0 \leqslant v \leqslant 1$; when $n = 0$ the superscripts are ignored. Inversion of (2.4) yields expansions of the form

$$\tau^{\pm}(v) = \sum_{k=1}^{\infty} \frac{a_{kn}^{\pm}}{\Gamma(\mu_n k + 1)} (\mathrm{e}^{-\mathrm{i}\theta}\omega_n v)^{\mu_n k}, \quad \mu_n = \begin{cases} \frac{1}{2} & (n = 0), \\ 1 & (n \geqslant 1) \end{cases} \tag{2.5}$$

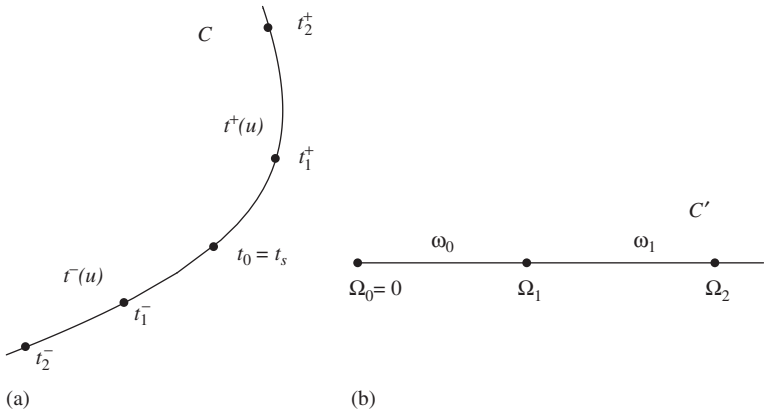

Fig. 1. (a) The subdivision of the steepest descent path C passing through the saddle point t_s and (b) the corresponding subdivision of C' in the u-plane.

valid in a certain disc about $u = \Omega_n$. The coefficients $a_{kn}^{\pm}$ satisfy $a_{k0}^{\pm} = (\pm 1)^k a_{k0}$, with the particular value $a_{10} = (\pi/2\psi''(t_s))^{1/2}$, and $a_{1n}^{\pm} = 1/\psi'(t_n^{\pm})$ for $n \geqslant 1$. The coefficients $a_{kn}^{\pm}$ can be determined either by the Lagrange inversion theorem [16, p. 133] or, in specific cases, by a numerical inversion procedure using *Mathematica*. Upon expansion of the amplitude function $f(t)$ about $t = t_n^{\pm}$, combined with (2.5), we then obtain

$$\left(f(t_n+\tau)\frac{\mathrm{d}t}{\mathrm{d}v}\right)^{\pm} = \omega_n \mathrm{e}^{-\mathrm{i}\theta}\sum_{k=0}^{\infty}\frac{c_{kn}^{\pm}}{\Gamma((k+1)\mu_n)}(\mathrm{e}^{-\mathrm{i}\theta}\omega_n v)^{(k+1)\mu_n-1}, \tag{2.6}$$

where

$$c_{k0}^{\pm} = (\pm 1)^{k-1} c_{k0}. \tag{2.7}$$

The first few coefficients $c_{kn}^{\pm}$ have the values

$$c_{0n}^{\pm} = a_{1n}^{\pm} f, \quad c_{1n}^{\pm} = a_{2n}^{\pm} f + \varepsilon_1 (a_{1n}^{\pm})^2 f',$$
$$c_{2n}^{\pm} = a_{3n}^{\pm} f + 3\varepsilon_2 a_{1n}^{\pm} a_{2n}^{\pm} f' + \varepsilon_3 (a_{1n}^{\pm})^3 f'', \ldots,$$

where f and its derivatives are evaluated at $t_n^{\pm}$ and $\varepsilon_1 = 2/\pi$, $\varepsilon_2 = \frac{1}{2}$, $\varepsilon_3 = 1/\pi$ $(n = 0)$, $\varepsilon_1 = \varepsilon_2 = \varepsilon_3 = 1$ $(n \geqslant 1)$. The $c_{kn}^{\pm}$ are seen to be explicitly independent of $\theta = \arg z$; however, there is an implicit dependence through the variation of the steepest descent path C with θ.

2.1. Hadamard expansions for $J(z)$ corresponding to different paths C

Each of the expansions in (2.6) is valid in a disc centered at $u = \Omega_n$ whose radius is controlled either by the nearest adjacent saddle point or singularity of $f(t)$ in the case $n = 0$ or (in the simplest situation) by the saddle t_s when $n \geqslant 1$. Provided the intervals ω_n are chosen so that the expansions (2.6) are used in their respective discs of convergence, we find that the contribution to the integral $J(z)$ from the intervals between $t_n^{\pm}$ and $t_{n+1}^{\pm}$ $(n = 0, 1, 2, \ldots)$ is

$$\begin{aligned}
&\mathrm{e}^{-z\psi(t_s)}\int_{\Omega_n}^{\Omega_{n+1}} \mathrm{e}^{-|z|u}\left(f(t)\frac{\mathrm{d}t}{\mathrm{d}u}\right)^{\pm}\mathrm{d}u \\
&\quad = \mathrm{e}^{-z\psi(t_s)-\Omega_n|z|}\sum_{k=1}^{\infty}\frac{c_{kn}^{\pm}(\omega_n \mathrm{e}^{-\mathrm{i}\theta})^{(k+1)\mu_n}}{\Gamma((k+1)\mu_n)}\int_0^1 \mathrm{e}^{-|z|\omega_n v} v^{(k+1)\mu_n-1}\,\mathrm{d}v \\
&\quad = \mathrm{e}^{-z\psi(t_s)-\Omega_n|z|}\sum_{k=0}^{\infty}\frac{c_{kn}^{\pm}}{z^{(k+1)\mu_n}}P((k+1)\mu_n, \omega_n|z|),
\end{aligned} \tag{2.8}$$

where $P(a, x)$ is the normalised incomplete gamma function defined in (1.3) and μ_n is defined in (2.5).

When C is the path that commences at the saddle t_s and passes to infinity along the upper half $t^+(u)$ of the steepest descent path, we therefore obtain

$$J(z) = \mathrm{e}^{-z\psi(t_s)}\sum_{n=0}^{\infty}\mathrm{e}^{-\Omega_n|z|}S_n(z), \tag{2.9}$$

where $S_n(z)$ denotes the Hadamard series defined by

$$S_n(z) = \sum_{k=0}^{\infty}\frac{c_{kn}}{z^{(k+1)\mu_n}}P((k+1)\mu_n, \omega_n|z|) \tag{2.10}$$

and the coefficients $c_{kn} \equiv c_{kn}^{+}$. A similar expression holds for the integral commencing at t_s and passing to infinity along the lower half $t^-(u)$ of the steepest descent path; in this case $c_{kn} \equiv c_{kn}^{-}$. If the path C is infinite in both directions, then $J(z)$ is again described by (2.9) but with the coefficients in (2.10) given by $c_{kn} \equiv c_{kn}^{+} - c_{kn}^{-}$.

From (2.7) and (2.8), the contributions to $J(z)$ from the intervals between t_s and $t_1^{\pm}$ are, respectively,

$$\mathrm{e}^{-z\psi(t_s)}\sum_{k=0}^{\infty}\frac{(\pm 1)^{k-1}c_{k0}}{z^{(k+1)/2}}\,P\left(\tfrac{1}{2}k+\tfrac{1}{2},\omega_0|z|\right). \tag{2.11}$$

For the interval between t_1^- and t_1^+ containing the saddle point t_s, there is a cancellation of the odd terms in (2.11) to produce the zeroth-interval contribution given by

$$S_0(z)=2\sum_{k=0}^{\infty}\frac{c_{2k,0}}{z^{k+1/2}}\,P\left(k+\tfrac{1}{2},\omega_0|z|\right). \tag{2.12}$$

The modifications required when the path C is finite are straightforward.

It may be remarked that the standard Poincaré asymptotic expansion for $J(z)$ is obtained by replacing the upper limit of integration in (2.8) in the zeroth interval by $+\infty$. In the case of the saddle t_s being an internal point, this corresponds to the series in (2.12) with the normalised incomplete gamma functions replaced by unity, viz.

$$J(z)\sim 2\mathrm{e}^{-z\psi(t_s)}\sum_{k=0}^{\infty}\frac{c_{2k,0}}{z^{k+1/2}}\quad(z\to\infty)$$

valid in some sector.

In the simplest situation where the other saddles of $\psi(t)$ are sufficiently remote, so that they are not effective in the determination of the convergence intervals with $n\geqslant 1$, a routine calculation on the lines of that described in [8, Section 10.4] shows that the inversion coefficients $a_{kn}^{\pm}$ in (2.5) possess the large-k growth

$$a_{kn}^{\pm}=\mathrm{O}(k^{-3/2}\Gamma(\mu_n k+1)\Lambda_n^{-\mu_n k}).$$

The quantity Λ_0 is the distance in the u-plane from the saddle t_s to the nearest adjacent saddle and $\Lambda_n=\Omega_n$ $(n\geqslant 1)$. Provided that the singularities of $f(t)$ are similarly sufficiently distant, then $c_{kn}^{\pm}=\mathrm{O}(a_{k+1,n}^{\pm})$ for $k\gg 1$. From the behaviour $P(a,z)\sim z^a\mathrm{e}^{-z}/\Gamma(a+1)$ as $a\to+\infty$ obtained from (1.3), the decay of the late terms in (2.10) is consequently controlled by

$$\mathrm{e}^{-\omega_n|z|}k^{-3/2}(\omega_n/\Lambda_n)^{\mu_n(k+1)}\quad(k\to\infty). \tag{2.13}$$

This result shows that, provided $\omega_n\leqslant\Lambda_n$, the Hadamard series in (2.10) are absolutely convergent.

We now discuss two different schemes for the selection of the interval lengths ω_n in the simplest case when the other saddles and possible singularities of the amplitude function are sufficiently remote to be ineffective in their determination when $n\geqslant 1$.

2.2. The forward-expansion procedure

The first scheme has been extensively described in I and here is called the *forward-expansion procedure*. This corresponds to choosing ω_n to be the radii of convergence of the expansions in (2.6); that is, we set $\omega_0=\Lambda_0$ and $\omega_n=\Omega_n$ $(n\geqslant 1)$ and expand about the left-hand endpoints $t_s, t_1^{\pm}, t_2^{\pm},\ldots$ (with maps at the points $u=0,\Omega_1,\Omega_2,\ldots$). This choice maximises the exponential separation between the different levels in (2.9) but at the cost of a slower rate of convergence of each Hadamard series in (2.10). This follows from the estimate in (2.13) which shows that in this case the late terms in the series $S_n(z)$ decay like $k^{-3/2}$.

As described in I, this slow algebraic decay of the tail of $S_n(z)$ can be transformed into a rapid decay comparable with the asymptotic-like phase of the early terms by a simple rearrangement of the tail. We write

$$S_n(z)=\sum_{k=0}^{M_n-1}\frac{c_{kn}}{z^{(k+1)\mu_n}}\,P((k+1)\mu_n,\omega_n|z|)+T_n(M_n;z), \tag{2.14}$$

where $c_{kn} \equiv c_{kn}^{\pm}$ and M_n are suitably chosen truncation indices. Upon use of (1.3), the tail T_n is given by

$$T_n(M_n; z) = \sum_{k=M_n}^{\infty} \frac{c_{kn}}{z^{(k+1)\mu_n}} P((k+1)\mu_n, \omega_n|z|) = \mathrm{e}^{-\omega_n|z|} \sum_{r=0}^{\infty} \sigma_{rn} \chi_n^r, \tag{2.15}$$

where $\chi_n = \omega_n|z|/M_n$. The coefficients σ_{rn} are [9]

$$\begin{aligned} \sigma_{rn} &= M_n^r \sum_{k=M_n}^{\infty} \frac{c_{kn}(\omega_n \mathrm{e}^{-\mathrm{i}\theta})^{(k+1)\mu_n}}{((k+1)\mu_n + r)!} \\ &= M_n^r \left\{ \frac{1}{r!} \int_{t_n^{\pm}}^{t_{n+1}^{\pm}} (1 - v_n)^r f(t)\, \mathrm{d}t - \sum_{k=0}^{M_n - 1} \frac{c_{kn}(\omega_n \mathrm{e}^{-\mathrm{i}\theta})^{(k+1)\mu_n}}{((k+1)\mu_n + r)!} \right\}, \end{aligned} \tag{2.16}$$

where, from (2.4), the variable $v_n \equiv v_n(t)$ is

$$v_n = \frac{\psi(t) - \psi(t_n^{\pm})}{\omega_n \mathrm{e}^{-\mathrm{i}\theta}} \quad (n = 0, 1, 2, \ldots). \tag{2.17}$$

The expression of $S_n(z)$ as a finite main sum, truncated after M_n terms, plus a rapidly convergent tail is called the *modified Hadamard series*. It is important to realise that the rearrangement of the tail in (2.15) and (2.16) is still exact and that no approximation has been introduced. We remark that T_n contains the exponentially small factor $\exp(-\omega_n|z|)$, which indicates the level of its contribution to $S_n(z)$, and that the coefficients σ_{rn} have a common form at each level n. In numerical calculations, the series for T_n is truncated after N_n terms compatible with the desired level of accuracy.

A variation of the forward-expansion procedure is to use interval lengths $\omega_n < \Lambda_n$, so that from (2.13) the convergence of the Hadamard series $S_n(z)$ is much more rapid. In this case, the exponential separation between the different levels in (2.9) is no longer maximal but, if the ω_n are suitably chosen, it is possible to avoid the separate evaluation of the tail given in (2.15) and (2.16). This represents a considerable saving in effort since it is the determination of the coefficients σ_{rn} that is the most computationally expensive part of the process.

2.3. The reverse-expansion procedure

The second scheme, which we call the *reverse-expansion procedure*, uses a suitably chosen set of interval lengths ω_n but expands about the right-hand endpoints $t_1^{\pm}, t_2^{\pm}, \ldots$. To illustrate, let us consider the case when the integration path C in (1.1) commences at the saddle t_s and passes to infinity along one of the halves of the steepest descent path. Then, instead of commencing by expanding about t_s as in the first scheme, we expand about a point $t_1^{\pm}$ chosen arbitrarily[3] on the steepest descent path so that

$$\omega_0 = \Omega_1 = \mathrm{e}^{\mathrm{i}\theta}\{\psi(t_1^{\pm}) - \psi(t_s)\}.$$

In the simplest case, the radius of convergence about $t_1^{\pm}$ will be controlled by the saddle at t_s and is consequently given by ω_0. The contribution to $J(z)$ from the interval t_s to $t_1^{\pm}$ now becomes

$$\begin{aligned} \mathrm{e}^{-z\psi(t_s)} \int_0^{\Omega_1} \mathrm{e}^{-|z|u} \left(f(t) \frac{\mathrm{d}t}{\mathrm{d}u} \right)^{\pm} \mathrm{d}u &= \mathrm{e}^{-z\psi(t_s) - \Omega_1|z|} \int_{-1}^{0} \mathrm{e}^{-|z|\omega_0 v} \left(f(t) \frac{\mathrm{d}t}{\mathrm{d}v} \right)^{\pm} \mathrm{d}v \\ &= -\mathrm{e}^{-z\psi(t_s) - \Omega_1|z|} \sum_{k=0}^{\infty} \frac{c_{k,1}^{\pm}}{z^{k+1}} P(k+1, -\omega_0|z|), \end{aligned}$$

where we have put $u = \Omega_1 + \omega_0 v$, with $-1 \leqslant v \leqslant 0$. We then continue this process by expanding about a sequence of *suitably chosen* points $t_n^{\pm}$ $(n \geqslant 2)$ on the steepest descent path and evaluating the contribution to $J(z)$ from

[3] This choice is actually a compromise between a desired exponential separation and the rate of convergence of the tail of the zeroth series; see [9].

$t_n^{\pm}$ to $t_{n-1}^{\pm}$ (that is, from Ω_n to Ω_{n-1} in the u-plane). This yields the expansion for $J(z)$ in the form

$$J(z) = \mathrm{e}^{-z\psi(t_s)} \sum_{n=0}^{\infty} \mathrm{e}^{-\Omega_n|z|} \mathbf{S}_n(z), \tag{2.18}$$

where the Hadamard series $\mathbf{S}_n(z)$ of the second kind are defined by

$$\mathbf{S}_n(z) = -\mathrm{e}^{-\omega_n|z|} \sum_{k=0}^{\infty} \frac{c_{k,n+1}^{\pm}}{z^{k+1}} P(k+1, -\omega_n|z|) \tag{2.19}$$

and the coefficients $c_{k,n+1}^{\pm}$ are specified by (2.6). We observe that at each step in this procedure we expand about the point $u = \Omega_n$ $(n \geqslant 1)$ in the u-plane and evaluate the contribution to $J(z)$ from the interval $[\Omega_{n-1}, \Omega_n]$, rather than from the interval $[\Omega_n, \Omega_{n+1}]$ as in the first scheme.

By the same argument leading to (2.13), the decay of the terms in $\mathbf{S}_n(z)$ can be shown to be controlled by

$$k^{-3/2}(\omega_n/\Omega_{n+1})^{k+1} \quad (k \to \infty);$$

we note the omission of the exponential factor in this estimate. For the zeroth interval, we have $\omega_0 = \Omega_1$; the decay of the late terms of $\mathbf{S}_0(z)$ is then controlled by the slow algebraic decay $k^{-3/2}$ and the analogue of the modified form of the expansion in (2.14) is required. This is given by

$$\mathbf{T}_0(M_0; z) = -\mathrm{e}^{-\omega_0|z|} \sum_{k=M_0}^{\infty} \frac{c_{k1}^{\pm}}{z^{k+1}} P(k+1, -\omega_0|z|) = \sum_{r=0}^{\infty} \hat{\sigma}_{r0}(-\chi_0)^r, \tag{2.20}$$

where

$$\begin{aligned} \hat{\sigma}_{r0} &= M_0^r \sum_{k=M_0}^{\infty} \frac{c_{k1}^{\pm}(-\omega_0 \mathrm{e}^{-\mathrm{i}\theta})^{k+1}}{(k+r+1)!} \\ &= M_0^r \left\{ \frac{1}{r!} \int_{t_0}^{t_1^{\pm}} v_0^r f(t)\, \mathrm{d}t + \sum_{k=0}^{M_0-1} \frac{c_{k1}^{\pm}(-\omega_0 \mathrm{e}^{-\mathrm{i}\theta})^{k+1}}{(k+r+1)!} \right\} \end{aligned} \tag{2.21}$$

and χ_0 and v_0 are specified in (2.15) and (2.17); see III. For the intervals with $n \geqslant 1$, however, we are at liberty to choose ω_n satisfying

$$\omega_n/\Omega_{n+1} = \vartheta < 1, \tag{2.22}$$

so that we may then benefit from the geometric rate of decay $k^{-3/2}\vartheta^{k+1}$ present in the late terms of $\mathbf{S}_n(z)$. If $\vartheta \simeq \frac{1}{2}$, for example, it is found that the terms in $\mathbf{S}_n(z)$ $(n \geqslant 1)$ decay sufficiently rapidly without the need to employ their modified form as described above for the zeroth-order contribution $\mathbf{S}_0(z)$.

A different version of the reverse-expansion procedure was employed in [9,14] to deal with coalescence of a neighbouring saddle point with the saddle t_s as some parameter in $\psi(t)$ varies. The reverse-expansion procedure was employed for the zeroth interval only, with the forward-expansion procedure being adopted for the remaining intervals with $n \geqslant 1$. This hybrid manner[4] of expansion was used to overcome the problem associated with the progressive loss of exponential separation between the different levels in the Hadamard expansion (2.9) as the zeroth interval $\omega_0 \to 0$ due to coalescence. A similar problem is encountered in the treatment of the Stokes phenomenon; see II.

In the following sections we present a series of examples illustrating the application of the above theory in situations involving poles of $f(t)$. In each case we supply numerical examples to demonstrate the accuracy that can be obtained.

[4] It is obvious that the reverse-expansion procedure could also be employed in the coalescence problem.

3. A Laplace integral with nearly coincident poles

As our first example consider the Laplace integral [3]

$$J(x) = \int_0^\infty \mathrm{e}^{-xt} f(t)\,\mathrm{d}t, \quad f(t) = \{(t-\mathrm{e}^{\mathrm{i}\phi})(t-\mathrm{e}^{-\mathrm{i}\phi})\}^{-1} \tag{3.1}$$

for large positive x when $0<\phi<\frac{1}{2}\pi$. The amplitude function $f(t)$ has simple poles at $t=\mathrm{e}^{\pm\mathrm{i}\phi}$ which straddle the integration path near $t=1$ for small values of ϕ; see Fig. 2. The standard Poincaré asymptotic expansion of $J(x)$ can be obtained by use of the Maclaurin expansion of $f(t)$, valid in $|t|<1$, followed by application of Watson's lemma (see, for example, [8, p. 113]) to yield

$$J(x) \sim \sum_{k=0}^\infty \frac{\sin(k+1)\phi}{\sin\phi}\,\frac{k!}{x^{k+1}} \quad (x\to+\infty). \tag{3.2}$$

As $\phi\to 0^+$, the calibre of this expansion degrades due to the proximity of the poles at $t=\mathrm{e}^{\pm\mathrm{i}\phi}$ to the integration path. To overcome this difficulty, the integration path in (3.1) can be deformed to pass either above or below one of the poles yielding a residue term in addition to the Poincaré series (3.2). Such a modification will be exploited in the Hadamard expansion process for $J(x)$.

Let α be an acute angle satisfying $0<\phi<\alpha<\frac{1}{2}\pi$. From the residue theorem, we can rotate the integration path $[0,\infty)$ to the ray $[0,\infty\mathrm{e}^{\mathrm{i}\alpha})$ resulting in

$$J(x) = \frac{\pi}{\sin\phi}\exp(-x\mathrm{e}^{\mathrm{i}\phi}) + \mathrm{e}^{\mathrm{i}\alpha}\int_0^\infty \mathrm{e}^{-zu} f(u\mathrm{e}^{\mathrm{i}\alpha})\,\mathrm{d}u \quad (z\equiv x\mathrm{e}^{\mathrm{i}\alpha}). \tag{3.3}$$

We now subdivide the positive real u-axis in the integral on the right-hand side of (3.3) into intervals of length ω_n $(n=0,1,2,\ldots)$ with left-hand endpoints Ω_n as defined in (2.2), where $\Omega_0=0$ and $\omega_0=\Omega_1=1$. Define the set of complex numbers $\Delta_n^\pm$ by

$$\Delta_n^\pm = \mathrm{e}^{\mathrm{i}(\pm\phi-\alpha)} - \Omega_n; \tag{3.4}$$

these quantities represent the separation between the endpoints Ω_n and the poles $u=\mathrm{e}^{\mathrm{i}(\phi-\alpha)}$ and $u=\mathrm{e}^{-\mathrm{i}(\phi+\alpha)}$, respectively; see Fig. 2. It is readily seen that $|\Delta_0^\pm|=1$ and $|\Delta_n^+|<|\Delta_n^-|$ $(n\geqslant 1)$. Then, since the pole at $u=\mathrm{e}^{\mathrm{i}(\phi-\alpha)}$ controls the discs of convergence on the integration path in $J(x)$, we set

$$\omega_n = |\Delta_n^+| \quad (n=0,1,2,\ldots). \tag{3.5}$$

With $u=\Omega_n+\omega_n v$, $0\leqslant v\leqslant 1$, we find upon some straightforward algebra the expansion

$$f(u\mathrm{e}^{\mathrm{i}\alpha}) = \frac{f(\Omega_n\mathrm{e}^{\mathrm{i}\alpha})}{(1-u/\Delta_n^+)(1-u/\Delta_n^-)} = \sum_{k=0}^\infty \mathrm{e}^{\mathrm{i}\alpha}\frac{c_{kn}}{k!}(\omega_n v)^k \quad (|v|<1),$$

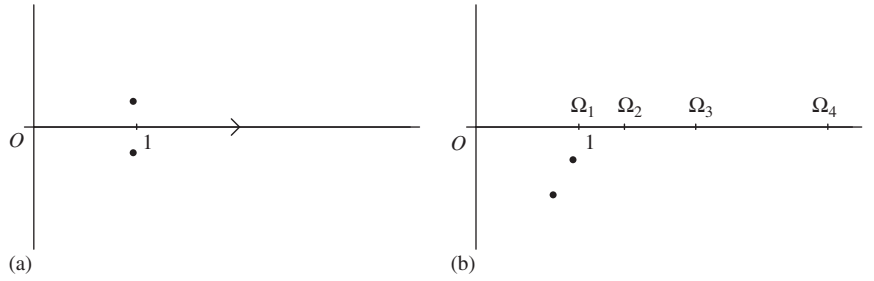

Fig. 2. The integration path in (a) the t-plane and (b) the u-plane. The heavy dots denote the poles at $\mathrm{e}^{\pm\mathrm{i}\phi}$ in the t-plane and at $\mathrm{e}^{\mathrm{i}(\pm\phi-\alpha)}$ in the u-plane.

where the coefficients $c_{kn} \equiv c_{kn}(\phi;\alpha)$ are determined explicitly by

$$c_{kn} = \frac{\mathrm{i}k!}{2\sin\phi}\left\{\left(\frac{\mathrm{e}^{-\mathrm{i}\alpha}}{\Delta_n^+}\right)^{k+1} - \left(\frac{\mathrm{e}^{-\mathrm{i}\alpha}}{\Delta_n^-}\right)^{k+1}\right\}. \tag{3.6}$$

From (3.3) and (2.8)–(2.10), we then obtain the Hadamard expansion

$$J(x) = \frac{\pi}{\sin\phi}\exp(-x\mathrm{e}^{\mathrm{i}\phi}) + \sum_{n=0}^{\infty}\mathrm{e}^{-\Omega_n z}S_n(z), \tag{3.7}$$

where $S_n(z)$ denotes the nth Hadamard series given by

$$S_n(z) = \sum_{k=0}^{\infty}\frac{c_{kn}}{x^{k+1}}\,P(k+1,\omega_n z) \quad (z \equiv x\mathrm{e}^{\mathrm{i}\alpha}). \tag{3.8}$$

At the zeroth level $n=0$ (where $\Omega_0 = 0$ and $\omega_0 = 1$), the coefficients c_{k0} simplify considerably and we find

$$S_0(x) = \sum_{k=0}^{\infty}\frac{k!\sin(k+1)\phi}{x^{k+1}\sin\phi}\,P(k+1,z). \tag{3.9}$$

If the incomplete gamma functions $P(k+1,z)$ are formally replaced by unity, then (3.9) reduces to the Poincaré expansion in (3.2). From (3.6) and the large-a behaviour of $P(a,x)$ used in (2.13), we find the behaviour of the late terms of $S_n(z)$ given by

$$\frac{\mathrm{i}\mathrm{e}^{-\omega_n z}}{2(k+1)\sin\phi}\left\{\left(\frac{\omega_n}{\Delta_n^+}\right)^{k+1} - \left(\frac{\omega_n}{\Delta_n^-}\right)^{k+1}\right\} \quad (k\to\infty). \tag{3.10}$$

Since $\omega_0/\Delta_0^{\pm} = \mathrm{e}^{\mathrm{i}(\alpha\mp\phi)}$ and $\omega_n/|\Delta_n^+| = 1$, $\omega_n/|\Delta_n^-| < 1$ $(n\geqslant 1)$, it follows that the Hadamard series in (3.8), in contrast to other expansions developed in I–III, are only conditionally convergent.

The modified form of expansion for $S_n(z)$ is given by (2.14) and (2.15). From (2.16), the coefficients σ_{rn} are determined by

$$\sigma_{rn} = M_n^r\sum_{k=M_n}^{\infty}c_{kn}\frac{(\omega_n\mathrm{e}^{\mathrm{i}\alpha})^{k+1}}{(k+r+1)!},$$

where M_n is the truncation index specified in (2.14). In this case, these may be evaluated explicitly as the difference between two Gauss hypergeometric functions in the form

$$\sigma_{rn} = \frac{\mathrm{i}M_n^r}{2\sin\phi}\,\frac{M_n!}{(M_n+r+1)!}\left\{F_{rn}\left(\frac{\omega_n}{\Delta_n^+}\right) - F_{rn}\left(\frac{\omega_n}{\Delta_n^-}\right)\right\}, \tag{3.11}$$

where for notational convenience[5]

$$F_{rn}(z) \equiv z^{M_n+1}\,{}_2F_1(1, M_n+1; M_n+r+2; z).$$

This follows from use of (3.6) and the easily established result, for positive integer m and $r\geqslant 0$,

$$\sum_{k=m}^{\infty}\frac{k!z^k}{(k+r+1)!} = z^m\sum_{k=0}^{\infty}\frac{(k+m)!z^k}{(k+m+r+1)!} = \frac{z^m m!}{(m+r+1)!}\,{}_2F_1(1,m+1;m+r+2;z).$$

To illustrate the procedure numerically, we choose the values $x=10$, $\phi = 0.07\pi$ and a path rotation of $\alpha = \pi/5$ and employ the forward-expansion procedure with maximal exponential separation determined by (3.5). In Fig. 3 we show

[5] We note that a number of so-called linear transformations can be applied to ${}_2F_1$ to produce different representations of the coefficients σ_{rn}. For example, a more suitable evaluation of F_{rn} for modest values of r can be achieved through the formula [1, Eq. (15.3.4)].

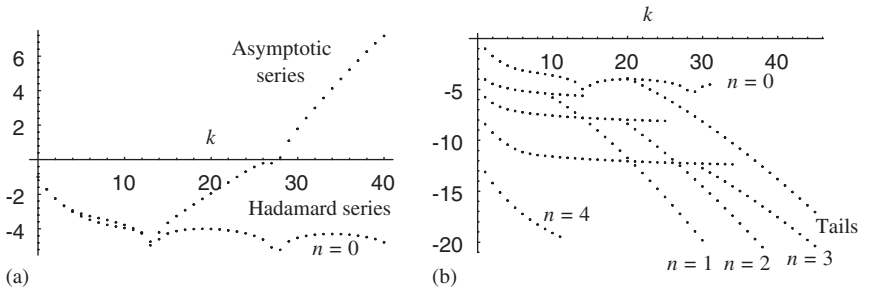

Fig. 3. Magnitude of the terms (on a $\log_{10}$ scale) against ordinal number k in the Hadamard series in (3.7) when $x = 10$, $\phi = 0.07\pi$ and $\alpha = \pi/5$: (a) comparison of the terms in $S_0(z)$ with those in the asymptotic series (3.2) and (b) the terms in the first four levels using the forward-expansion procedure with maximal exponential separation.

Table 1
Absolute values of the error in $J(x)$ when $x = 10$ and $\phi = 0.07\pi$ at different levels

n	ω_n	Approximation to $J(x)$	|Error|
0	1.0000	0.129**4**3599782458696712**4**	9.167×10^{-4}
1	0.4056	0.129345**4**65545916507824	1.580×10^{-6}
2	0.6290	0.12934513**0**827694130150	3.531×10^{-9}
3	1.1854	0.1293451314917**3**0609113	7.397×10^{-14}
4	2.3362	0.12934513149171850492**8**	3.317×10^{-21}
	Exact	0.12934513149171850492**9**	

The truncation indices employed are indicated in the text.

an example of the magnitude of the terms in the first levels of the expansion (3.7). The first figure shows a comparison of the magnitude of the terms in the Poincaré series (3.2) and the zeroth-level Hadamard series $S_0(x)$. The series of 'spikes' on these latter terms is caused by near-zeros of the term $\sin(k+1)\phi$ and the logarithmic scale employed in the figures. We demonstrate the numerical accuracy that can be achieved with this procedure in Table 1, with the truncation indices $(M_0, N_0) = (20, 30)$, $(M_1, N_1) = (10, 21)$, $(M_2, N_2) = (25, 20)$ and $M_4 = 12$ (with no tail at level $n = 4$), where N_n refers to the truncation index of the tail T_n. The exact value of $J(x)$ was obtained from the representation in terms of the exponential integral $E_1(z)$ [1, Eq. (5.1.1)] in the form

$$J(x) = \frac{1}{\sin\phi}\mathrm{Im}\{\mathrm{e}^{-x\mathrm{e}^{\mathrm{i}\phi}} E_1(-x\mathrm{e}^{\mathrm{i}\phi})\} \quad (x > 0;\ \phi \neq 0).$$

We remark that optimal truncation of the Poincaré series in (3.2) yields an accuracy of order 10^{-5} with the above values of x and ϕ.

For values of ϕ bounded well away from 0, the poles at $t = \mathrm{e}^{\pm\mathrm{i}\phi}$ have less influence on the integral and the development of the Hadamard expansion can proceed without any preliminary path rotation to produce the expansion in (3.7) with $\alpha = 0$ and the residue term deleted. As $\phi \to 0^+$, however, the discs of convergence for $n \geqslant 1$ have radius $\omega_n \to 0$, with the consequence that the Hadamard expansion for $J(x)$ will suffer from a progressive loss of exponential separation between the different levels after the zeroth level. In this limit, the rotated integration path offers a more well-differentiated set of exponential levels.

Another possible choice of integration path in (3.1) would be to take the directed line segment $[0, \mathrm{e}^{\mathrm{i}\alpha}]$ followed by the ray $[\mathrm{e}^{\mathrm{i}\alpha}, \mathrm{e}^{\mathrm{i}\alpha} + \infty)$ parallel to the real t-axis. An advantage with such a 'cranked' path is that on the horizontal path the integration variable has constant imaginary part which will result in incomplete gamma functions of positive argument in the Hadamard series in (3.8) with $n \geqslant 1$. For complex values of the second argument, $|P(a, z)|$ loses its characteristic 'cut-off' behaviour and displays some oscillation, a feature that will result in a slight loss of overall accuracy. Such calculations are reported in [3], where it was found with the above values of x and ϕ that a more significant factor in deciding which contour to choose was the difference in the exponential levels Ω_n $(n \geqslant 1)$ in the two cases. Simple

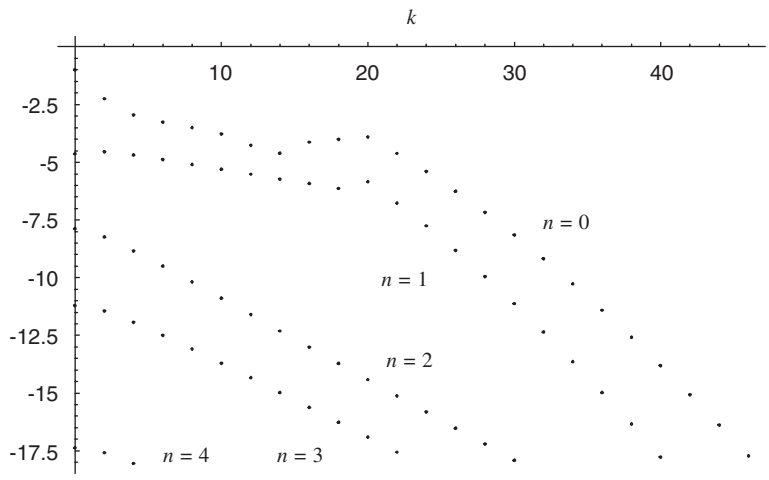

Fig. 4. Magnitude of the terms (on a $\log_{10}$ scale) against ordinal number k in the Hadamard series in (3.12) when $x = 10$, $\phi = 0.07\pi$ and $\alpha = \pi/5$ using the reverse-expansion procedure with $\omega_1 = \omega_2 = 0.8$, $\omega_3 = 1.6$.

geometrical considerations reveal that, for a given path rotation α, the exponential separation between the different levels with $n \geqslant 1$ is greater with the rotated path than with the 'cranked' path.

Finally, a different expansion procedure can be adopted if it is desired to keep the rotation angle α reasonably small. This uses a slight modification of the reverse-expansion procedure discussed in Section 2.3. For the rotated path, the zeroth interval $[0, \mathrm{e}^{\mathrm{i}\alpha}]$ is the same as before, with expansion $S_0(z)$; the remainder of the path is then dealt with by the reverse-expansion procedure with conveniently chosen intervals $\omega_1, \omega_2, \ldots$. From (2.18), the resulting Hadamard expansion for $J(x)$ then takes the form

$$J(x) = \frac{\pi}{\sin\phi}\exp(-x\mathrm{e}^{\mathrm{i}\phi}) + \sum_{n=0}^{\infty} \mathrm{e}^{-\Omega_n z}\mathbf{S}_n(z), \tag{3.12}$$

where, for convenience, we have set $\mathbf{S}_0(x) = S_0(x)$ as defined in (3.9) and the Hadamard series of the second kind $\mathbf{S}_n(z)$ are given by

$$\mathbf{S}_n(z) = -\mathrm{e}^{-\omega_n z}\sum_{k=0}^{\infty} \frac{c_{k,n+1}}{x^{k+1}}\, P(k+1, -\omega_n z) \quad (n \geqslant 1); \tag{3.13}$$

compare (2.19). The modified form of the tail of $\mathbf{S}_n(z)$ when truncated after M_n terms is, from (2.20), given by

$$\mathbf{T}_n(M_n; z) = \sum_{r=0}^{\infty} \hat{\sigma}_{rn}(-\chi_n)^r, \quad \chi_n = \omega_n z/M_n \quad (n \geqslant 1).$$

The coefficients $\hat{\sigma}_{rn}$, which are defined in an analogous manner to the first sum in (2.21), can be evaluated explicitly in terms of hypergeometric functions in the form

$$\hat{\sigma}_{rn} = -\frac{\mathrm{i}M_n^r}{2\sin\phi}\,\frac{M_n!}{(M_n+r+1)!}\left\{F_{rn}\left(-\frac{\omega_n}{\Delta_{n+1}^+}\right) - F_{rn}\left(-\frac{\omega_n}{\Delta_{n+1}^-}\right)\right\},$$

where F_{rn} is defined at (3.11).

By means of a similar argument to that used in (3.10), the late terms in $\mathbf{S}_n(z)$ are ultimately controlled by $(-\omega_n/\Delta_{n+1}^+)^{k+1}k^{-1}$. At level $n = 1$, we have $\omega_1 \lesssim |\Delta_2^+|$ so that the series $\mathbf{S}_1(z)$ will exhibit the familiar slow convergence and use of the modified form with tail $\mathbf{T}_1(M_1; z)$ will be necessary. For the other levels corresponding to $n \geqslant 2$, however, it is possible to choose ω_n such that $\omega_n/|\Delta_{n+1}^+| \lesssim \frac{1}{2}$, say. The resulting convergence of the unmodified series

Table 2
Absolute values of the error in $J(x)$ when $x = 10$ and $\phi = 0.07\pi$ at different levels using the reverse-expansion procedure for two different sets of ω_n values

n	ω_n	|Error|	ω_n	|Error|
0	1.000	9.087×10^{-5}	1.000	9.087×10^{-5}
1	0.800	3.256×10^{-8}	0.800	3.256×10^{-8}
2	0.800	4.040×10^{-12}	1.200	4.638×10^{-13}
3	1.600	9.455×10^{-18}	3.000	1.221×10^{-23}

The truncation indices employed in each case are indicated in the text.

$\mathbf{S}_n(z)$ is then seen to be geometric and evaluation of these series can be achieved without use of the modified form of the expansion.

To illustrate, we repeat the calculation of $J(x)$ for the values $x = 10$, $\phi = 0.07\pi$ and path rotation $\alpha = \pi/5$. We set $\omega_1 = \omega_2 = 0.8$ and $\omega_3 = 1.6$ and use the truncation indices $(M_0, N_0) = (20, 25)$, $(M_1, N_1) = (20, 20)$, $M_2 = 30$ and $M_3 = 22$ (with no tails at levels $n = 2, 3$). The magnitude of the terms in $\mathbf{S}_n(z)$ for $0 \leqslant n \leqslant 3$ is shown in Fig. 4; the first few terms in $\mathbf{S}_4(z)$ are also indicated but are not used in the calculations. It is plainly seen that the series at levels $n = 2$ and 3 decay rapidly and that modification is not necessary. The results of the computations are presented in Table 2, where we also display a second set of ω_n values with greater exponential separation and truncation indices $(M_0, N_0) = (20, 35)$, $(M_1, N_1) = (25, 25)$ and values of M_2, M_3 compatible with the desired level of accuracy. Comparison of the results in Tables 1 and 2 shows that a greater accuracy can be achieved with the reverse-expansion procedure with fewer levels than with the forward-expansion procedure with ω_n given by (3.5).

4. A Laplace-type integral with nearly coincident poles and saddles

In our second example we consider the Laplace-type integral

$$J(x) = \int_0^\infty \mathrm{e}^{-x\psi(t)} f(t)\,\mathrm{d}t,$$

where the phase and amplitude functions are given by

$$\psi(t) = \frac{1}{3}t^3 - a^2 t + \frac{2}{3}a^3, \quad f(t) = \frac{t^2}{t^2 + (\kappa a)^2} \tag{4.1}$$

with the parameters $a \geqslant 0$ and $\kappa > 0$. The exponential factor has two saddle points at $t = \pm a$ and the amplitude function has two simple poles at $t = \pm \mathrm{i}\kappa a$, as shown in Fig. 5. The phase function is normalised such that $\psi(a) = 0$. As $a \to 0^+$, the saddles and the poles approach the endpoint of integration $t = 0$ as a cluster to produce a double saddle at the origin (with $f(t) \equiv 1$) when $a = 0$.

It will be found convenient to divide the range of integration into the intervals $[0, a]$ and $[a, \infty)$ and to denote the corresponding contributions to the integral by I_1 and I_2, respectively. We consider the interval $[0, a]$ first and expand about the saddle $t = a$. The associated coefficients c_{k0} are specified by an expansion of the form (2.6) with $\psi(t)$ and $f(t)$ given in (4.1). The radius ω of the disc of convergence about $t = a$ is

$$\omega = \min\{\psi(-a),\ |\psi(\pm \mathrm{i}\kappa a)|\} = \min\left\{\frac{4}{3}a^3,\ \left|\frac{2}{3}a^3 \mp \mathrm{i}\kappa a^3\left(1 + \frac{1}{3}\kappa^2\right)\right|\right\}.$$

It is easily verified that ω is determined by the poles at $t = \pm \mathrm{i}\kappa a$ when $0 < \kappa < \kappa_0$, where $\kappa_0 \doteq 0.90644$, and by the saddle at $t = -a$ when $\kappa > \kappa_0$. From (2.11) and recalling that $\psi(a) = 0$, we accordingly obtain the single Hadamard expansion for I_1 in the form

$$I_1 = \int_0^a \mathrm{e}^{-x\psi(t)} f(t)\,\mathrm{d}t = \sum_{k=0}^\infty \frac{(-)^k c_{k0}}{x^{(k+1)/2}}\, P\left(\tfrac{1}{2}k + \tfrac{1}{2}, \hat{\omega}_0 x\right), \tag{4.2}$$

where $\hat{\omega}_0 = \psi(0) - \psi(a) = \frac{2}{3}a^3$ $(< \omega)$.

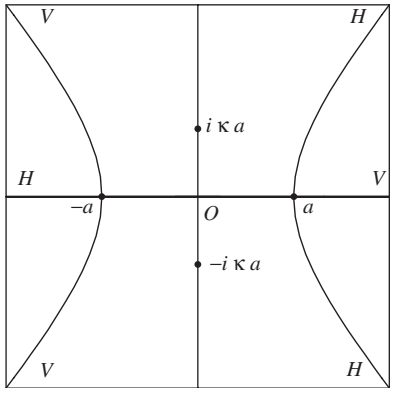

Fig. 5. The steepest descent and ascent paths for the phase function $\psi(t)$ in (4.1). The saddle points at $\pm a$ and the poles of $f(t)$ at $\pm i\kappa a$ are denoted by heavy dots. The valleys (V) and hills (H) at infinity are indicated.

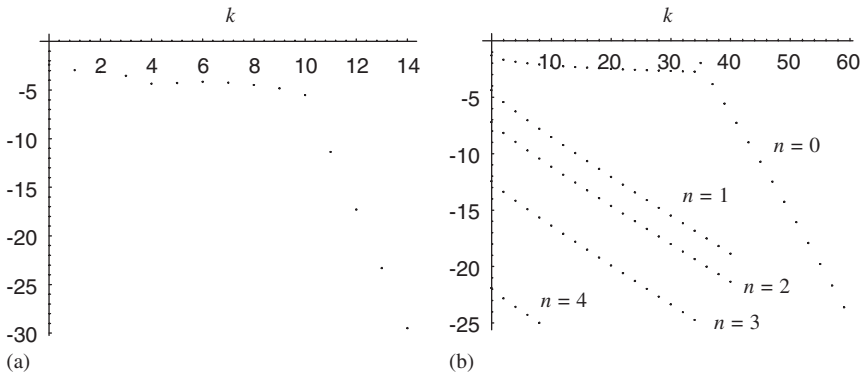

Fig. 6. Magnitude of the terms (on a $\log_{10}$ scale) against ordinal number in the Hadamard series for (a) I_1 and (b) I_2 using the reverse-expansion procedure when $x = 20$, $a = 10^{-2}$ and $\kappa = 1$.

When a is finite, the forward-expansion procedure discussed in Section 2.2 can be used to evaluate the contribution from the interval $[a, \infty)$, where the zeroth interval length ω_0 is set equal to ω. This procedure has been discussed in I, II and is not considered any further here. In the small-a limit, $\omega \to 0$ and the reverse-expansion procedure must be used to avoid loss of exponential separation in the resulting Hadamard expansion. We expand about a suitably chosen sequence of points t_n $(n \geqslant 1)$, with $t_s = a$. In terms of the variable $u = \psi(t)$, this sequence corresponds to the points $u = \Omega_n = \psi(t_n)$, and so defines a set of intervals in the u-plane of length $\omega_n = \Omega_{n+1} - \Omega_n$ $(n \geqslant 0)$; cf. Fig. 1(b). With the coefficients c_{kn} specified by an expansion of the form (2.6) about Ω_n $(n \geqslant 1)$, we obtain from (2.18) the Hadamard expansion

$$I_2 = \int_a^\infty \mathrm{e}^{-x\psi(t)} f(t)\,\mathrm{d}t = \sum_{n=0}^\infty \mathrm{e}^{-\Omega_n x}\,\mathbf{S}_n(x), \tag{4.3}$$

where $\Omega_0 = 0$ and, from (2.19),

$$\mathbf{S}_n(x) = -\mathrm{e}^{-\omega_n x} \sum_{k=0}^\infty \frac{c_{k,n+1}}{x^{k+1}}\, P(k+1, -\omega_n x).$$

As a numerical illustration we set $x = 20$ and $\kappa = 1$. For I_1 and the zeroth level in I_2, we employ the modified form of these expansions given in (2.14), (2.15), (2.20) and (2.21). The computation of I_2 is carried out using four levels, with $t_1 = 1.00$, $t_2 = 1.24$, $t_3 = 1.54$ and $t_4 = 1.90$, which correspond to the values $\Omega_1 \doteq 0.3333$, $\Omega_2 \doteq 0.6355$, $\Omega_3 \doteq 1.2174$

Table 3
Absolute values of the error in $J(x)$ for different values of a and κ when $x = 20$

κ	$a = 10^{-1}$	$a = 10^{-2}$	$a = 10^{-4}$
0.5	4.417×10^{-19}	1.753×10^{-19}	1.715×10^{-19}
1.0	3.887×10^{-19}	1.738×10^{-19}	1.715×10^{-19}
2.0	2.944×10^{-19}	1.734×10^{-19}	1.715×10^{-19}

The truncation indices employed are indicated in the text.

and $\Omega_4 \doteq 2.2863$. This choice of intervals agrees with the requirements of the reverse-expansion procedure with $\vartheta \simeq 0.475$ stated in (2.22). The decay of the terms against ordinal number k is illustrated in Fig. 6 for the particular case $a = 10^{-2}$ and $\kappa = 1$. It is seen again that the terms in levels with $n \geqslant 1$ for I_2 decay sufficiently rapidly without the need to employ the modified form of the series. In Table 3 we give the absolute error in the computation of $J(x)$ for different values of a. The truncation indices employed[6] are $(M_0, N_0) = (10, 2)$ for I_1 and $(M_0, N_0) = (30, 20)$, $M_1 = M_2 = 40$, $M_3 = 20$ for I_2.

5. A Laplace-type integral with a pole in the phase factor

In this section we consider the Laplace-type integral

$$J(x) = \int_{-\infty+ic}^{\infty+ic} \mathrm{e}^{-x\psi(t)} f(t)\,\mathrm{d}t \quad (c > 0), \tag{5.1}$$

where the phase and amplitude functions are given by

$$\psi(t) = t^2 + \frac{2}{t} - 3\mathrm{e}^{-2\pi\mathrm{i}/3}, \quad f(t) = 1, \tag{5.2}$$

$x > 0$ and the integration path is taken parallel to the real axis; see [4, p. 52]. The phase function has a pole at $t = 0$ and three saddles on the unit circle situated at $t = 1, \mathrm{e}^{\pm 2\pi\mathrm{i}/3}$. The saddles at $t = \mathrm{e}^{\pm 2\pi\mathrm{i}/3}$ are of unit height, while the saddle at $t = 1$ has height $-3(1 - \mathrm{e}^{-2\pi\mathrm{i}/3})$ and so is subdominant. The steepest descent paths through the saddles are illustrated in Fig. 7; with $c > 0$, the integration path can be deformed to pass over the saddles at $t = \mathrm{e}^{2\pi\mathrm{i}/3}$ and $t = 1$, approaching the pole at $t = 0$ in a direction situated in $\mathrm{Re}(t) > 0$.

We introduce the new variable given by $u = \psi(t) - \psi(t_s)$, where t_s denotes either of the saddles at $\mathrm{e}^{2\pi\mathrm{i}/3}$ or 1. The presence of the pole results in a division of the steepest descent path into two separate halves, on each of which u runs from 0 to ∞. For each steepest descent path, we then select a suitable sequence of values of ω_n (and hence, by (2.2), the levels Ω_n) and determine the corresponding values of $t_n^{\pm}$ by solution of (2.3). Inversion of (2.4) yields the coefficients $c_{kn}^{\pm}$ in (2.6) for each path. Then, from (2.9), (2.10) and (2.12), it follows that $J(x)$ can be written as the sum of two expansions about the saddles $t_s = \mathrm{e}^{2\pi\mathrm{i}/3}$, 1 of the form

$$\mathrm{e}^{-x\psi(t_s)} \sum_{k=0}^{\infty} \mathrm{e}^{-\Omega_n x} S_n(x),$$

where

$$S_n(x) = \sum_{k=0}^{\infty} \frac{C_{kn}}{x^{k+\mu_n}} P(k + \mu_n, \omega_n x)$$

with $C_{k0} = 2c_{2k,0}$, $C_{kn} = c_{kn}^{+} - c_{kn}^{-}$ $(n \geqslant 1)$ and μ_n is defined in (2.5).

In this example, we apply the forward-expansion procedure with the interval lengths ω_n chosen to be less than the radii of convergence[7] about the points $t_n^{\pm}$. For the dominant saddle $t_s = \mathrm{e}^{2\pi\mathrm{i}/3}$, we choose levels with $n \leqslant 3$ given by

[6] When $a = 10^{-1}$ the truncation indices for I_1 were taken as $(M_0, N_0) = (10, 5)$.

[7] For example, with $\omega_0 = 2$ on the steepest descent path containing the dominant saddle $t_s = \exp(2\pi\mathrm{i}/3)$, it is easily verified that the points $t_1^{\pm}$ at the extremities of the zeroth interval are situated inside the unit circle centered at t_s.

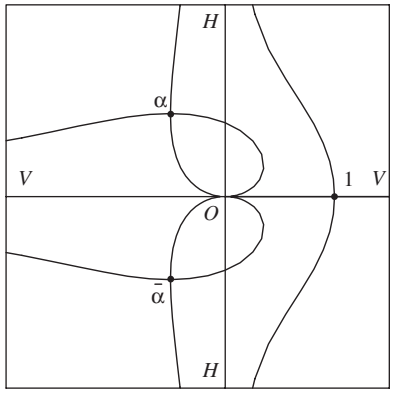

Fig. 7. The steepest descent and ascent paths for the phase function in (5.2). The saddle points are denoted by heavy dots with $\alpha = \exp(2\pi i/3)$. The valleys (V) and hills (H) at infinity are indicated.

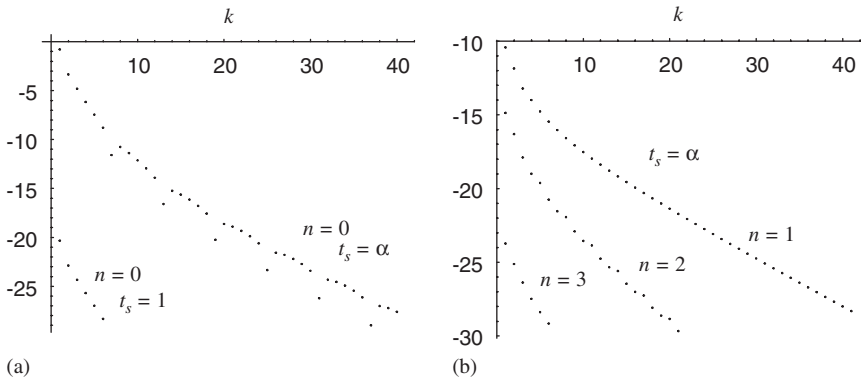

Fig. 8. Magnitude of the terms (on a $\log_{10}$ scale) against ordinal number k in the Hadamard series for $J(x)$ at different levels with $x = 10$: (a) the terms in the zeroth series containing the saddles at $t_s = \alpha$ $(=e^{2\pi i/3})$ and $t_s = 1$ and (b) the terms in levels $1 \leqslant n \leqslant 3$ on the positive side of the saddle at $t_s = \alpha$.

$\omega_0 = 2$, $\omega_1 = 1$, $\omega_2 = 2$ and $\omega_3 = 1$ (so that $\Omega_0 = 0$, $\Omega_1 = 2$, $\Omega_2 = 3$, $\Omega_3 = 5$ and $\Omega_4 = 6$). For the subdominant saddle $t = 1$ we use only the zeroth interval and choose $\omega_0 = 2$. The results of computations with $x = 10$ are shown in Fig. 8. In the first figure we display the behaviour of the terms (on a logarithmic scale) in each of the zeroth Hadamard series $\exp\{-x\psi(t_s)\}S_0(x)$ containing the dominant and subdominant saddles. In the second figure we display the terms in the Hadamard series at levels $1 \leqslant n \leqslant 3$ on the positive side of the dominant saddle; the terms on the negative side possess a similar behaviour. It is seen that with our choice of intervals ω_n, the terms at each level exhibit a rapid decay, so that high-precision evaluation of $J(10)$ can be achieved without the need for employing the modified form of expansions given in (2.14)–(2.16). In the computations, we truncated the series $S_n(10)$ after M_n terms, where $M_0 = M_1 = 40$, $M_2 = 20$ and $M_3 = 5$ for the dominant saddle, and $M_0 = 5$ for the subdominant saddle. The value of $J(10)$ from the Hadamard expansion was compared with that obtained from high-precision numerical quadrature of (5.1) with $c = \frac{1}{2}$ and the absolute error was found to be 3.059×10^{-28}.

6. A Laplace-type integral with a pole approaching a saddle

In our final example we examine the effect of a simple pole approaching a stationary saddle point. We consider the integral (1.1) with $\psi(t) = t^2 - 2it$, $f(t) = 1/(t^2 + a^2)$, where a is a positive parameter satisfying $a \leqslant 1$, and the

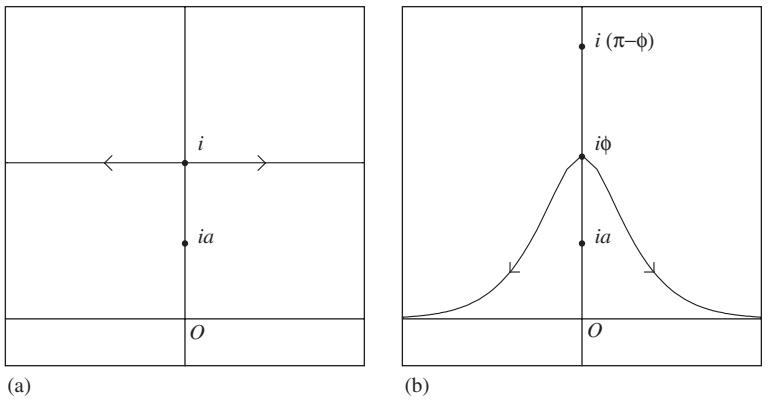

Fig. 9. The steepest descent path through the saddle t_s when (a) $\psi(t) = t^2 - 2it$, $t_s = \mathrm{i}$ and (b) $\psi(t) = \cosh t - it\sin\phi$, $t_s = \mathrm{i}\phi$ (when $\phi < \frac{1}{2}\pi$). The arrows denote the direction of descent and the pole of $f(t)$ at $t = \mathrm{i}a$ is also indicated.

integration path C is the real axis $(-\infty, \infty)$ [4, p. 60]. We therefore have

$$J(x) = \mathrm{e}^{-x}\int_{-\infty}^{\infty} \mathrm{e}^{-x(t-\mathrm{i})^2}\,\frac{\mathrm{d}t}{t^2+a^2}, \tag{6.1}$$

where x will be assumed to be a large positive variable. The exponential factor has a saddle point at $t_s = \mathrm{i}$ and the amplitude function has simple poles at $t = \pm\mathrm{i}a$ on the imaginary axis. The steepest descent path through t_s is the line parallel to the real t-axis; see Fig. 9(a). We are primarily concerned here with the case when the pole $\mathrm{i}a$ is close to the saddle.

When $a < 1$, the integration path can be displaced over the pole at $t = \mathrm{i}a$ and made to coincide with the steepest descent path through t_s, to yield

$$J(x) = \frac{\pi}{a}\,\mathrm{e}^{-a(2-a)x} + \mathrm{e}^{-x}\int_{-\infty+\mathrm{i}}^{\infty+\mathrm{i}} \mathrm{e}^{-x(t-\mathrm{i})^2}\,\frac{\mathrm{d}t}{t^2+a^2} \quad (a<1). \tag{6.2}$$

In the limit $a \to 1$ we use the reverse-expansion procedure, since expansion of the integrand about t_s will result in a circle of convergence controlled by the nearby pole at $t = \mathrm{i}a$. With the new variable $u = (t-\mathrm{i})^2$, we choose the intervals ω_n so that the exponential levels Ω_n are determined from (2.2). The radii of convergence of the series expansion (2.6) about the points $t_n = \mathrm{i} + \sqrt{\Omega_n}$ is

$$\min\{|\psi(t_n) - \psi(t_s)|, |\psi(t_n) - \psi(\pm\mathrm{i}a)|\} = \min\{\Omega_n, \Omega_n + (1 \mp a)^2\}$$

and so is controlled by the saddle point. From (2.18) and (6.2), the Hadamard expansion of $J(x)$ is then given by

$$J(x) = \frac{\pi}{a}\mathrm{e}^{-a(2-a)x} + 2\mathrm{e}^{-x}\mathrm{Re}\sum_{n=0}^{\infty}\mathrm{e}^{-\Omega_n x}\,\mathbf{S}_n(x) \quad (a<1), \tag{6.3}$$

where $\mathbf{S}_n(x)$ is the Hadamard series of the second kind defined in (2.19).

In numerical computations, we take $x = 10$ and use two levels with the intervals $\omega_0 = 2$, $\omega_1 = 2$ (so that $\Omega_0 = 0$, $\Omega_1 = 2$). For the zeroth level we employ the modified form of $\mathbf{S}_0(x)$ given in (2.20) and (2.21). The above choice of ω_1 yields the parameter $\vartheta \simeq \frac{1}{2}$ in (2.22) for the interval with $n = 1$. The decay of the terms in the sum in (6.3) against ordinal number k is shown in Fig. 10(a) for the particular case $a = 0.9$. The error was obtained by comparison with the exact evaluation of $J(x)$ given by

$$J(x) = \frac{\pi}{2a}\mathrm{e}^{-x}(E_1 + E_2),$$

where $E_j = \mathrm{e}^{\lambda_j^2 x}\{1 + (-)^{j-1}\mathrm{erf}(\lambda_j x^{\frac{1}{2}})\}$, $\lambda_j = 1 + (-)^j a$ and erf denotes the error function.

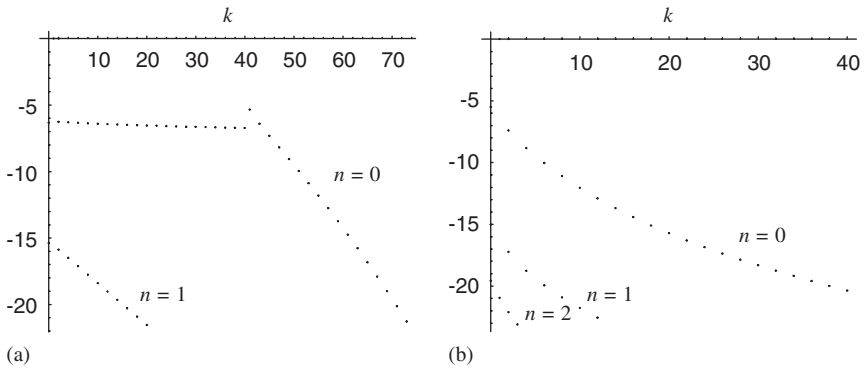

Fig. 10. Magnitude of the terms (on a $\log_{10}$ scale) against ordinal number k when $x = 10$ in the Hadamard expansions (a) in (6.3) with $a = 0.9$ and (b) in (6.5) with $a = 1$.

When $a = 1$ the pole in the upper half-plane becomes coincident with the saddle point. In this case, we take the integration path in (6.2) to be the same horizontal line, $\mathrm{Im}(t) = 1$, but indented *above* the point $t = \mathrm{i}$ and adopt the approach discussed in [15]. We apply the forward-expansion procedure with suitably chosen intervals ω_n. In this simple example we have $\mathrm{d}t/\mathrm{d}u = \frac{1}{2}u^{-1/2}$ and so obtain the expansion about $t = \mathrm{i}$ in the form

$$\left(f(t)\frac{\mathrm{d}t}{\mathrm{d}u}\right)^{\pm} = \frac{1}{4\mathrm{i}u}\left(1 \pm \frac{u^{1/2}}{2\mathrm{i}}\right)^{-1} = \frac{1}{4\mathrm{i}u} + \sum_{k=0}^{\infty} \frac{(\pm)^{k-1}c_{k0}}{\Gamma(\frac{1}{2}k+\frac{1}{2})}u^{(k-1)/2}, \tag{6.4}$$

where the coefficients c_{k0} are given explicitly by $c_{k0} = 2^{-k-3}\mathrm{i}^k\Gamma(\frac{1}{2}k+\frac{1}{2})$. The radius of convergence of this expansion is controlled by the pole at $t = -\mathrm{i}$ and is valid in $|u| < 4$; this means that we must choose $\omega_0 \leqslant 4$. The indented integration path corresponds to a negatively orientated loop[8] in the u-plane surrounding the positive real u-axis. As a consequence, the term $(4\mathrm{i}u)^{-1}$ contributes $-\frac{1}{2}\pi\mathrm{e}^{-x}$ to the integral in (6.2) which, with the residue term of $\pi\mathrm{e}^{-x}$ (when $a = 1$), yields the contribution $\frac{1}{2}\pi\mathrm{e}^{-x}$. From (6.2), we then obtain the Hadamard expansion

$$J(x) = \frac{1}{2}\pi\mathrm{e}^{-x} + 2\mathrm{e}^{-x}\mathrm{Re}\sum_{n=0}^{\infty}\mathrm{e}^{-\Omega_n x}S_n(x) \quad (a = 1), \tag{6.5}$$

where, from (2.10),

$$S_n(x) = \sum_{k=0}^{\infty}\frac{c_{kn}}{x^{(k+1)\mu_n}}P((k+1)\mu_n, \omega_n x)$$

and μ_n is defined in (2.5).

The choice of the intervals ω_n in (6.5) can be made according to two schemes. The first uses maximal exponential separation with the ω_n taken equal to the associated radii of convergence, namely $\omega_0 = \omega_1 = 4$, $\omega_2 = 8$, $\omega_3 = 16, \ldots$; in this case it would be necessary to employ the modified form of the Hadamard series in (2.14) and (2.15) at each level. The second choice uses values of ω_n somewhat less than the associated radii of convergence such that the parameter $\vartheta \simeq \frac{1}{2}$ in (2.22). In this case the Hadamard series $S_n(x)$ will converge rapidly *at each level* and the modified form is not required. In the calculations, we adopted the second alternative and used the levels $0 \leqslant n \leqslant 2$ with $\omega_0 = 2$, $\omega_1 = 1$ ($\vartheta = \frac{1}{2}$) and $\omega_2 = 1$ ($\vartheta = \frac{1}{3}$). The decay of the terms in the sum (6.5) against ordinal number k is displayed in Fig. 10(b). The values of the absolute error in the computation of $J(x)$ for different values of a in the limit $a \to 1$ when $x = 10$ are presented in Table 4. The truncation indices employed are $(M_0, N_0) = (40, 30)$, $M_1 = 20$ for $a < 1$ and $M_0 = 40$, $M_1 = 10$, $M_2 = 2$ when $a = 1$.

[8] If the indentation had been below the point $t = \mathrm{i}$, the contour in the u-plane would be a positively orientated loop.

Table 4
Absolute values of the error in $J(x)$ in (6.1) for different values of a when $x = 10$

$1-a$	|Error|
10^{-1}	4.930×10^{-21}
10^{-2}	2.022×10^{-23}
10^{-3}	5.451×10^{-22}
10^{-4}	5.972×10^{-22}
0	2.539×10^{-21}

The truncation indices employed are indicated in the text.

We make a remark at this point concerning the computation of the modified form of the Hadamard series $\mathbf{S}_0(x)$ which is employed when $a < 1$. The coefficients $\hat{\sigma}_{r0}$ in (2.21) involve the evaluation of the integrals

$$\int_{t_0}^{t_1^{\pm}} v_0^r f(t)\,\mathrm{d}t,$$

where $v_0(t)$ is defined in (2.17) and $t_0 \equiv t_s$. Since $v_0(t_0) = 0$, it is seen that for $r \geqslant 1$ the effect of the singularity in $f(t)$, which approaches t_0 as $a \to 1$, is diluted by the presence of the term v_0^r. However, when $r = 0$, this effect is no longer present and, to avoid loss of numerical precision, it is better to evaluate the integral in $\hat{\sigma}_{00}$ explicitly.

The same procedure can be applied to the integral

$$\int_{-\infty}^{\infty} \mathrm{e}^{-x(\cosh t - \mathrm{i}t\sin\phi)} \frac{\mathrm{d}t}{t^2+a^2} \quad \left(0 \leqslant \phi \leqslant \frac{1}{2}\pi\right),$$

for example. Not surprisingly, this integral presents a richer structure than that in (6.1). The exponential factor now has an infinite string of saddle points on the imaginary axis, with the main saddle at $t_s = \mathrm{i}\phi$ and the two adjacent saddles situated at $t = \mathrm{i}(\pm\pi - \phi)$ (when $\phi < \frac{1}{2}\pi$). When $\phi = \frac{1}{2}\pi$, pairs of saddles coalesce to form a string of double saddles at $t = (2k + \frac{1}{2})\pi\mathrm{i}$, $k = 0, \pm 1, \pm 2, \ldots$. The steepest descent path through the saddle t_s is illustrated in Fig. 9(b) along which the integration path may be deformed. For the situations $a < \phi < \frac{1}{2}\pi$ and $a = \phi < \frac{1}{2}\pi$, the reverse-expansion and forward-expansion procedures (with an indented contour), respectively, can be employed as for the integral in (6.1).

However, as $\phi \to \frac{1}{2}\pi$, the forward-expansion procedure used when $a = \phi$ would be hampered by the presence of the approaching adjacent saddle at $t = \mathrm{i}(\pi - \phi)$. In this case we could employ a combination of expansion about t_s, as in (6.4) to extract the pole contribution with the convergence interval ω_0 controlled by the saddle $\mathrm{i}(\pi - \phi)$, followed by the reverse-expansion procedure applied to the remainder of the steepest descent path. We do not discuss this integral any further here.

7. Concluding remarks

We have introduced two basic modes of expansion using Hadamard series, namely the forward- and reverse-expansion procedures. The first scheme uses the Hadamard series $S_n(z)$, defined in (2.10), and is suitable for isolated saddle points when adjacent saddles or other singularities are sufficiently remote to result in a sequence of well-separated exponential levels. If maximal exponential separation is employed, the resulting convergence of the Hadamard series has to be accelerated through use of the modified form of the series. This involves the computation of coefficients expressed in terms of one-dimensional integrals of a common form at each level of the expansion.

If one is prepared to accept a reduced exponential separation, however, it is possible, through judicious choice of the exponential levels, to produce Hadamard series that converge rapidly without the need for the modified form. This second scheme is indispensable for coalescence problems and involves the Hadamard series of the second kind $\mathbf{S}_n(z)$ defined in (2.19). This mode of expansion avoids the loss of exponential separation that results in the forward-expansion procedure when either another saddle or singularity approaches the saddle point under consideration. The zeroth interval in the reverse-expansion procedure requires use of the modified form of $\mathbf{S}_0(z)$ to accelerate convergence, with the series in the remaining intervals converging sufficiently rapidly to make the modified form unnecessary.

To conclude, we make three remarks on the different nature of the Hadamard series $S_n(z)$ and $\mathbf{S}_n(z)$. First, the normalised incomplete gamma function $P(k+1, -\omega_n|z|)$ appearing in $\mathbf{S}_n(z)$ has no branch-point structure for nonnegative

integer k and consequently assumes real values. Secondly, the late terms in $\mathbf{S}_n(z)$ are roughly a factor $\exp(\omega_n|z|)$ larger than the corresponding terms in $S_n(z)$ $(n \geqslant 1)$ since, by application of the result $P(a, z) \sim z^a \mathrm{e}^{-z}/\Gamma(1+a)$ as $a \to +\infty$, we have the simple estimate for integer k

$$\frac{\mathrm{e}^{-\omega_n|z|} P(k+1, -\omega_n|z|)}{P(k+1, \omega_n|z|)} \sim (-)^{k+1} \mathrm{e}^{\omega_n|z|} \quad (k \to \infty).$$

This difference in the magnitude of the terms in $S_n(z)$ and $\mathbf{S}_n(z)$ can be displayed alternatively by noting that

$$\frac{P(k+1, X)}{X^{k+1}} = \frac{1}{k!} \int_0^1 \tau^k \mathrm{e}^{-X\tau} \, \mathrm{d}\tau,$$

$$\frac{\mathrm{e}^{-X} P(k+1, -X)}{(-X)^{k+1}} = \frac{1}{k!} \int_0^1 (1-\tau)^k \mathrm{e}^{-X\tau} \, \mathrm{d}\tau$$

and by observing that the maximum values of the integrands occur at $\tau = 1$ (when $k \geqslant X$) and $\tau = 0$ (for all $k \geqslant 0$), respectively. And thirdly, although the terms in $\mathbf{S}_n(z)$ are an exponential level greater than those in $S_n(z)$, the *rates of decay* of the terms in the two types of Hadamard series are found numerically to be comparable.

References

[1] M. Abramowitz, I.A. Stegun, Handbook of Mathematical Functions, Dover, New York, 1965.
[2] W. Gautschi, F.E. Harris, N.M. Temme, Expansions of the exponential integral in incomplete gamma functions, Appl. Math. Lett. 16 (2003) 1095–1099.
[3] D. Kaminski, R.B. Paris, Hadamard expansions for a Laplace integral with nearly coincident poles, Technical Report MS 03:03, University of Abertay Dundee, 2003.
[4] H.A. Lauwerier, Asymptotic Expansions, Mathematical Centre Tracts 13, Amsterdam, 1966.
[5] S.D. Lin, H.M. Srivastava, Fractional calculus and its applications involving bilateral expansions and multiple infinite sums, J. Fract. Calculus 25 (2004) 47–58.
[6] C. Morosi, L. Pizzocchero, On the expansion of the Kummer function in terms of incomplete gamma functions, Arch. Inequalities Appl. 2 (2004) 49–72.
[7] K.E. Muller, Computing the confluent hypergeometric function, Numer. Math. 90 (2001) 179–196.
[8] F.W.J. Olver, Asymptotics and Special Functions, Academic Press, New York, 1974; A.K. Peters, Massachusets, 1997, reprinted.
[9] R.B. Paris, Exactification of the method of steepest descents: the Bessel functions of large order and argument, Proc. Roy. Soc. London A 460 (2004) 2737–2759.
[10] R.B. Paris, On the use of Hadamard expansions in hyperasymptotic evaluation of Laplace-type integrals: I. Real variable, J. Comput. Appl. Math. 167 (2004) 293–319.
[11] R.B. Paris, On the use of Hadamard expansions in hyperasymptotic evaluation of Laplace-type integrals: II. Complex variable, J. Comput. Appl. Math. 167 (2004) 321–343.
[12] R.B. Paris, On the use of Hadamard expansions in hyperasymptotic evaluation of Laplace-type integrals: III. Clusters of saddle points, J. Comput. Appl. Math., to appear.
[13] R.B. Paris, D. Kaminski, Hadamard expansions for integrals with saddles coalescing with an endpoint, Appl. Math. Lett. 18 (2005) 1389–1395.
[14] R.B. Paris, D. Kaminski, Hyperasymptotic evaluation of the Pearcy integral via Hadamard expansions, J. Comput. Appl. Math. 190 (2006) 437–452.
[15] B.L. Van der Waerden, On the method of saddle points, Appl. Sci. Res. Ser. B 2 (1950) 33–45.
[16] E.T. Whittaker, G.N. Watson, A Course of Modern Analysis, Cambridge University Press, Cambridge, 1952.
[17] S. Yang, H.M. Srivastava, Some generalizations of the Hadamard expansion for the modified Bessel function, Appl. Math. Lett. 17 (2004) 591–596.